

# Relativistic evaluation of the two-photon decay of the metastable $1s^2 2s 2p^3 P_0$ state in berylliumlike ions with an effective-potential model

Pedro Amaro,<sup>1,\*</sup> Filippo Fratini,<sup>2</sup> Laleh Safari,<sup>3</sup> Jorge Machado,<sup>1,4</sup> Mauro Guerra,<sup>1</sup> Paul Indelicato,<sup>4</sup> and José Paulo Santos<sup>1</sup>

<sup>1</sup>Laboratório de Instrumentação, Engenharia Biomédica e Física da Radiação (LIBPhys-UNL), Departamento de Física, Faculdade de Ciências e Tecnologia, Universidade Nova de Lisboa, P-2829-516 Caparica, Portugal

<sup>2</sup>Atominstitut, Vienna University of Technology, A-1020 Vienna, Austria

<sup>3</sup>Institute of Science and Technology Austria, Am Campus 1, A-3400 Klosterneuburg, Austria

<sup>4</sup>Laboratoire Kastler Brossel, Sorbonne University, Univ. Pierre et Marie Curie-Paris 06, École Normale Supérieure, Collège de France, CNRS, Case 74, 4 place Jussieu, F-75005 Paris, France

(Received 10 September 2015; revised manuscript received 8 January 2016; published 7 March 2016)

The two-photon  $1s^2 2s 2p^3 P_0 \rightarrow 1s^2 s^2 {}^1S_0$  transition in berylliumlike ions is investigated theoretically within a fully relativistic framework and a second-order perturbation theory. We focus our analysis on how electron correlation, as well as the negative-energy spectrum, can affect the forbidden  $E1M1$  decay rate. For this purpose, we include the electronic correlation via an effective local potential and within a single-configuration-state model. Due to its experimental interest, evaluations of decay rates are performed for berylliumlike xenon and uranium. We find that the negative-energy contribution can be neglected at the present level of accuracy in the evaluation of the decay rate. On the other hand, if contributions of electronic correlation are not carefully taken into account, it may change the lifetime of the metastable state by up to 20%. By performing a fully relativistic  $jj$ -coupling calculation, we find a decrease of the decay rate by two orders of magnitude compared to nonrelativistic  $LS$ -coupling calculations, for the selected heavy ions.

DOI: [10.1103/PhysRevA.93.032502](https://doi.org/10.1103/PhysRevA.93.032502)

## I. INTRODUCTION

Two-photon decay has been studied experimentally and theoretically for many atomic systems since it was originally discussed by Göppert-Mayer [1]. In low- $Z$  atomic systems, the  $2s$ - $1s$  transitions in hydrogenlike and heliumlike ions occur primarily by two electric dipole photons ( $E1E1$ ) and the respective decay rates provided by theory and experiment are in good agreement. These works focused not only on the total and energy-differential decay rates [2–4], but also on the angular and polarization correlations of the two emitted photons [5–9]. Detailed analysis of these two-photon properties has been used to reveal unique information about electron densities in astrophysical plasmas and thermal x-ray sources, as well as highly precise values of physical constants [10]. The study of two-photon decay in high- $Z$  ions has also provided a sensitive tool for exploring the relativistic and quantum electrodynamic effects that occur in the strong atomic fields of those systems. As in the case of low- $Z$  ions, predictions for two-photon decay rates are in good agreement with experimental data [11–14].

Few investigations have been performed so far for *other* atomic systems with more than two electrons. In the case of lithiumlike ions, this lack of research might be attributed to almost all two-photon transitions being in direct competition with dominant allowed (single  $E1$ ) transitions, thus reducing the importance of the former processes in practical applications. However, this is not the case for berylliumlike ions with zero nuclear spin ( $I = 0$ ). Owing to the

$0 \rightarrow 0$  selection rule, the first excited state  $1s^2 2s 2p^3 P_0$  is metastable and its transition to the ground state  $1s^2 s^2 {}^1S_0$  is strictly forbidden for all single-photon multipole modes. The most dominant decay process is a rare two-photon transition with magnetic and electric dipole modes ( $E1M1$ ) that is very sensitive to relativistic and electronic correlation effects and can have lifetimes from a few decades to a few minutes, depending on the atomic electromagnetic field of the nucleus.

Knowledge of metastable decay rates is essential in collision-radiative modeling of astrophysical low-density plasmas that occur in stellar coronae [15]; thus many studies have been dedicated to the measurement and the calculation of higher-order ( $M1$  and  $E2$ ) and hyperfine-induced  $E1$  transitions modes [16–18]. Measurements of the metastable hyperfine-induced decay rate in  $N^{3+}$  was first performed at the Hubble Space Telescope with important implications to the isotopic abundance in an observed nebula [19]. The value of the  $E1M1$  decay rate in berylliumlike sulfur can also play an important role, specially because the majority of stable isotopes ( ${}^{32}S$  and  ${}^{34}S$ ) have nuclei with  $I = 0$  and have observable quantities in the solar coronae [18,20,21].

Besides this astrophysical interest, there is also motivation for calculating the  $E1M1$  two-photon decay mode coming from experiments aimed at testing the standard model via the observation of parity nonconservation in berylliumlike uranium [22,23]. Moreover, some unusual x-ray lines coming from an electron cyclotron resonance plasma might be attributed to charge state mechanisms involving the berylliumlike metastable state  $1s^2 2s 2p^3 P_0$  [24]. More recently, the  ${}^1S_0 \rightarrow {}^3P_0$   $E1M1$  transition in group-II-type atoms has also attracted attention as a possible way to design an atomic clock with advantages of portability and a Doppler-free excitation scheme [25].

\*pdamaro@fct.unl.pt

There are no experimental results for the  $E1M1$  decay rates in zero-spin berylliumlike ions available. Only recently, several dielectronic recombination resonances were clearly identified as coming from a parent  $1s^22s2p^3P_0$  metastable state in xenon ( $^{136}\text{Xe}^{+50}$  with  $I = 0$ ), which should lead to a measurement of the respective  $E1M1$  decay rate [26,27]. In these works, the need of fully relativistic calculations for this decay rate is emphasized.

In isotopes with nonzero  $I$  the importance of the  $E1M1$  mode is reduced: The hyperfine mixing between the term  $^3P_0$  and the closely lying above term  $^3P_1$  produces states with total angular momentum  $F \neq 0$ , thus circumventing the  $0 \rightarrow 0$  selection rule. This drastically reduces the lifetime of the metastable  $1s^22s2p^3P_0$  state since it opens an  $E1$  single-photon channel. Decay rates for this hyperfine-induced  $E1$  mode have been known theoretically for years [18,28–30] and the first measurements were performed recently, both in laboratory [31,32] and in a planetary nebula [19]. A review of this topic can be found in Ref. [33]. External magnetic and electric fields also induce the  $E1$  mode [23,34].

From the theoretical point of view, the calculation of this two-photon decay rate offers a challenge not only because berylliumlike ions have energy states separated by few percent of ionization energies, which makes electronic correlation of paramount importance, but also due to relativistic effects, such as the presence of the negative-energy continuum. Figure 1 illustrates the atomic structure in berylliumlike uranium, where the initial, (some) intermediate, and final states are drawn. Previous studies about two-photon decay with an  $M1$  component have shown that the negative-energy continuum contribution is mandatory for both low- $Z$  and high- $Z$  ions [35,36]. Furthermore, similar investigations in one-photon  $M1$  transitions have also shown an important contribution for high- $Z$  ions [37] and concluded that the inclusion of the negative-

energy continuum gives better agreement with experimental data [38] as well as improvements in gauge invariance [39–41]. Electronic correlation and relativistic effects (including a negative continuum) have to be efficiently incorporated in the second-order summation over the intermediate states that characterizes two-photon transitions.

Up to now, only two estimations of the  $E1M1$  decay rate for berylliumlike systems have been available [42,43], both assuming a nonrelativistic approximation and  $LS$ -coupling scheme, which for high- $Z$  ions may lead to significant deviations. Moreover, the summation over the intermediate states was restricted only to the first terms,  $1s^22s2p^3P_1$  and  $1s^22s2p^1P_1$ .

In this work we calculate the two-photon decay rate of the metastable  $1s^22s2p^3P_0$  state in berylliumlike ions by considering a *relativistic* evaluation of the second-order summation in a  $jj$ -coupling scheme and single-configuration model. Negative-energy states are thus included and their effect is investigated. In order to take into account the electronic correlation, we perform the evaluation of the second-order summation via a finite basis set and an effective local potential, with a few key intermediate-state energies calculated using the multiconfiguration Dirac-Fock (MCDF) method. For these evaluations, we consider berylliumlike xenon and uranium, following the reasoning above. For elements lighter than xenon, we notice that the strong electronic correlation prevents the present method from obtaining a reliable decay rate.

## II. THEORY

### A. General two-photon decay rate

The evaluation of two-photon related quantities have been discussed several times in the literature [11,12,44,45], therefore, we present here only a short compilation of expressions that are essential for further discussion of the influence of the relativistic and electronic correlation effects. Two-photon processes are evaluated following a second-order perturbation theory, which overall contains a summation over the complete spectrum of a given Hamiltonian. The differential decay rate of two-photon spontaneous emission between (many-electron) atomic states  $\Psi_i \rightarrow \Psi_f$ , obtained after summing over the photons polarizations and integrated over all possible emission directions, is given by

$$\begin{aligned} \frac{dW}{d\omega_1} &= \frac{\omega_1\omega_2}{(2\pi)^3c^2(2J_i+1)} \\ &\times \sum_{\substack{L_1M_1\lambda_1 \\ L_2M_2\lambda_2 \\ M_i,M_f}} \left| \sum_n \frac{\langle \Psi_f | \mathcal{T}_{L_2M_2}^{(\lambda_2)*} | \Psi_n \rangle \langle \Psi_n | \mathcal{T}_{L_1M_1}^{(\lambda_1)*} | \Psi_i \rangle}{E_n - E_i + \omega_1} \right. \\ &\left. + \frac{\langle \Psi_f | \mathcal{T}_{L_1M_1}^{(\lambda_1)*} | \Psi_n \rangle \langle \Psi_n | \mathcal{T}_{L_2M_2}^{(\lambda_2)*} | \Psi_i \rangle}{E_n - E_i + \omega_2} \right|^2, \end{aligned} \quad (1)$$

where the indices  $i$ ,  $f$ , and  $n$  stand for the initial, final, and intermediate states. The one-body transition operator  $\mathcal{T}_{L_jM_j}^{(\lambda_j)} = \sum_{i'} \tilde{a}_{L_jM_j}^{(\lambda_j)*}(\mathbf{r}_{i'})$  ( $j = 1, 2$ ) contains the interaction between each  $i'$  electron (with vector position  $\mathbf{r}_{i'}$ ) and the radiation field. Here  $\tilde{a}_{L_jM_j}^{(\lambda_j)}(\mathbf{r}_{i'})$  is the relativistic multipole of rank  $L_j$  of the

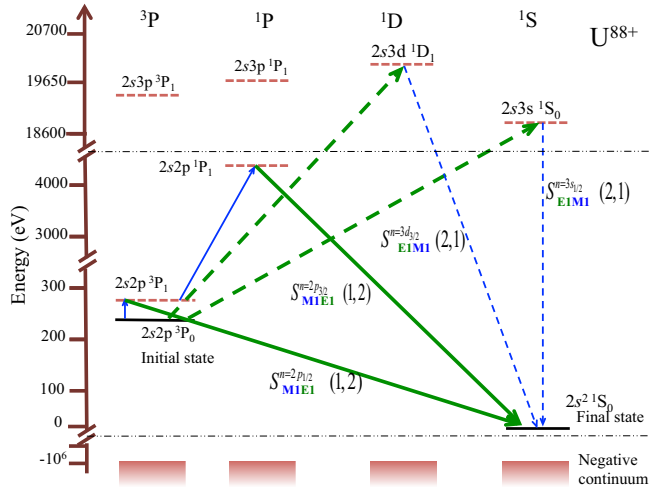


FIG. 1. Energy atomic structure of berylliumlike uranium relative to the final state  $2s^2 1S_0$ . The four paths composed of the blue ( $M1$ ) and thicker green ( $E1$ ) arrows connect the initial state to the final state, through the first intermediate states of  $S^{1/2}(2,1)$ ,  $S^{3/2}(2,1)$ ,  $S^{1/2}(1,2)$ , and  $S^{3/2}(1,2)$  of Eq. (2), which are allowed by selection rules. Solid and dashed arrows show the  $S^{j_n}(1,2)$  and  $S^{j_n}(2,1)$  amplitudes, respectively.

spherical-tensor expansion of the electron-photon interaction [11,46]. The values of  $\lambda$  are restricted to  $\lambda_j = \pm 1$  and to  $\lambda_j = 0$ , which addresses to electric  $EL_j$  and magnetic  $ML_j$  multipole types, respectively. The quantities  $\omega_1$  and  $\omega_2$  are the energies of the two emitted photons and  $c$  is the speed of light. Note that, differently from Eq. (1) in Ref. [45], there is an extra third power in  $\omega_1$  and  $\omega_2$ . This is a consequence of the electric dipole transition operator used in Ref. [45] being of length gauge type in a nonrelativistic limit (details in Ref. [46]).

Atomic states  $\Psi_q \equiv \Psi^q(J_q M_q)$  ( $q = i, f, n$ ) are usually given as a linear combination of (antisymmetrical)  $jj$ -coupled configuration-state functions (CSFs)  $\Phi_{klop}(J_q M_q)$  within a MCDF or configuration interaction (CI), where the four subscripts  $k, l, o$ , and  $p$  identify the orbitals,  $J_q$  is the total angular momentum, and  $M_q$  is its projection along the quantization axis. We hereby define an intermediate state with major contribution of a CSF with a spectator-orbital excitation ( $1s$  or  $2s$ ) as  $\Psi^{\text{exc}}(J_n M_n)$ . Here  $\Psi^{\text{nonexc}}(J_n M_n)$  are intermediate states where the major contribution addresses to a CSF  $\Phi_{1s^2 2s n' l'}(J_n M_n)$  with nonexcitation of the spectator orbitals. From now on we omit  $1s^2$  in configurations for brevity.

### B. Single-configuration model

In this work, only CSFs with variations of the active electron's quantum numbers  $n'l'_j$  that participates in the transition  $\Phi_{2s2p}(00) \rightarrow \Phi_{2s n' l'_j}(1M_n) \rightarrow \Phi_{2s^2}(00)$  are taken into account in the initial, intermediate, and final states, for the evaluation of Eq. (1). Other CSFs with excitation of the spectator electron are thus not taken into account. This is accomplished by considering the dominant single CSF in all states, as well as orthogonal orbitals. In order to better justify this model, we give in Fig. 2 a diagram of the allowed matrix elements involving one  $\Psi^{\text{exc}}(1M_n)$  and one  $\Psi^{\text{nonexc}}(1M_n)$ . Path (a) involves a state  $\Psi^{\text{nonexc}}(1M_n)$  with major contribution of  $\Phi_{2s2p}(1M_n)$ . This path is also represented in Fig. 1. Because the radiative operator  $\mathcal{T}_{L_j M_j}^{(\lambda)}$  is a one-body operator,  $\Psi^{\text{exc}}(1M_n)$  states give non-null matrix elements only by considering either path (b) or path (c) of Fig. 2.

*Path (b).* Electron orbitals are almost orthogonal between all states, thus if the radiative operator connects the active orbitals, there is a small contribution of  $\Psi^{\text{exc}}(1M_n)$  due to  $\langle 3s^n | 2s^f \rangle \neq 0$ , where  $3s^n$  and  $2s^f$  are spectator orbitals in the  $\Psi^{\text{exc}}(1M_n)$  and final state.

*Path (c).* The final and initial states can have a reasonable contribution of a configuration with the same spectator orbital as  $\Psi^{\text{exc}}(1M_n)$  due to configuration mixing, i.e.,  $\Psi_i(00) \approx c_0^i \Phi_{2s2p}(00) + c_1^i \Phi_{3s2p}(00)$  and  $\Psi_f(00) \approx c_0^f \Phi_{2s^2}(00) + c_1^f \Phi_{2s3s}(00)$ . The configuration coefficients can be obtained either by MCDF or CI methods.

These two cases show how a multiconfiguration approach and fully relaxed orbitals can play a role in two-photon processes by allowing  $\Psi^{\text{exc}}(1M_n)$  states beyond the assumption of only using CSFs with variations of the active electron participating in the transition.

For the present elements of xenon and uranium, MCDF calculations made for the initial, intermediate, and final states with fully relaxed orbitals and excited CSFs (all excitations

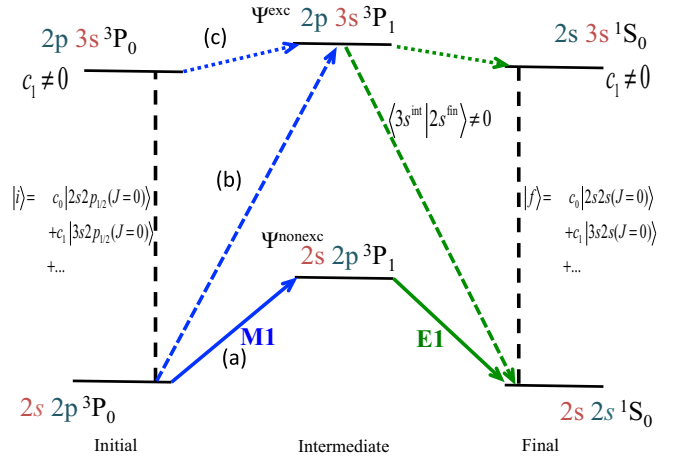


FIG. 2. Diagram of paths, or allowed matrix elements, connecting the initial state to the final state through  $\Psi^{\text{nonexc}}(1M_n)$  and  $\Psi^{\text{exc}}(1M_n)$  possible intermediate states. Blue and green arrows represent  $M1$  and  $E1$  multipoles, respectively. Path (a) (solid arrows) corresponds to an intermediate state  $\Psi^{\text{nonexc}}(1M_n)$  with a dominant contribution of  $\Phi_{2s2p}(1M_n)$ . Path (b) (dashed arrows) connects an intermediate state  $\Psi^{\text{exc}}(1M_n)$  to the final and initial states via the nonorthogonality of the spectator electrons. Path (c) (dot arrows) connects correlation configurations of the initial and final states to  $\Psi^{\text{exc}}(1M_n)$ . The dashed line means a link between the configurations with higher  $c_0$  and minor  $c_1$  contributions in the  $jj$  expansion.

of orbitals up to a principal number of 3) show results that justify the use of single CSFs with variations of the active electron. First, due to the strong field of the nucleus, even for xenon, the radial orbitals obtained for the spectator electrons are reasonably orthogonal in all initial, final, and intermediate states (residues of 2%). Second, the CSF mixing coefficients of both initial (99%  $2s2p_{1/2}$ ) and final states [98%  $2s^2 + 2%$  ( $2p_{1/2}^2$ ) $_0$ ] are well represented by a single CSF. Intermediate states have also a major contribution of a single CSF. For example, the two states  $(2s2p)_{J=1}$  have 99%  $2s2p_{1/2}$  and 99%  $2s2p_{3/2}$ , respectively.

For low- $Z$  ions or neutral beryllium, on the other hand, strong electron correlation does not allow the application of a single CSF for the atomic states. The intermediate-state summation can be done either via an inhomogeneous four-electron Dirac Hamiltonian (as in Ref. [12] for heliumlike ions) or by the introduction of  $\Psi^{\text{exc}}(1M_n)$ , which requires a careful analysis of the configuration mixing coefficients and orthogonality.

For the present case of the  $E1M1$  two-photon decay between the initial  $2s2p^3P_0$  and final  $2s^2^1S_0$  states (terms are given for state identification), the differential decay rate within a single CSF model is given by (in a.u.)

$$\frac{dW}{d\omega_1} = \frac{\omega_1 \omega_2}{(2\pi)^3 c^2} \sum_{\lambda=-1,1} \left| \sum_{j_n=1/2}^{3/2} [S^{j_n}(2,1) + S^{j_n}(1,2)] \right|^2, \quad (2)$$

where  $j_n$  is the total angular momentum of the active electron performing the transition  $2p \rightarrow n'l' j_n \rightarrow 2s$ . The sum of both photon energies is equal to the  $2s2p^3P_0 - 2s^2^1S_0$  energy difference to ensure energy conservation,  $E_{2s2p^3P_0} -$

$E_{2s^2 1S_0} = \omega_1 + \omega_2 = \omega_t$ . The two-photon amplitudes  $S^{jn}(2,1)$  and  $S^{jn}(1,2)$  contain the summation over the reduced matrix elements of the  $E1$  and  $M1$  multipole components, which are given by

$$S^{jn}(2,1) = \sum_n \frac{\langle 2s^1 S_0 || M_1(\omega_2) || n_\nu j_\nu \rangle \langle n_\nu j_\nu || E_1^\lambda(\omega_1) || 2p^3 P_0 \rangle}{E_n - E_{2s2p^3 P_0} + \omega_1}, \quad (3)$$

with the multipole components, electric dipole and magnetic dipole, being given by the relativistic radiative operators  $\tilde{a}_1^{(\lambda)*}(\mathbf{r}) \equiv E_1^\lambda(\omega)$  and  $\tilde{a}_1^{(0)*}(\mathbf{r}) \equiv M_1(\omega)$ , respectively. Explicit expressions of the reduced matrix elements are given in the Appendix. Here  $S^{jn}(1,2)$  is given by an equation similar to Eq. (3) by interchanging  $E_1^\lambda(\omega_1)$  with  $M_1(\omega_2)$  in the numerator and  $\omega_1$  with  $\omega_2$  in the denominator. We represent in Fig. 1 the first state of the summation allowed by selection rules for the four two-photon amplitudes  $S^{1/2}(2,1)$ ,  $S^{3/2}(2,1)$ ,  $S^{1/2}(1,2)$ , and  $S^{3/2}(1,2)$ , which are the  $2s3s_{1/2} 1S_0$ ,  $2s3d_{3/2} 1D_1$ ,  $2s2p_{1/2} 3P_1$ , and  $2s2p_{3/2} 1P_1$  states, respectively.

### C. Effective local potential

In the present model, the evaluation of the two-photon amplitudes is performed by applying the finite-basis-set (FBS) method to the representation of the active electron of the (single CSF)  $\Psi^{\text{nonexc}}(1M_n)$  intermediate states. A  $B$ -spline basis set [47,48] is considered for a cavity of radius 60 a.u. and 50 positive-energy and 50 negative-energy states. A degree of correlation is introduced in order to match the respective orbitals obtained by the MCDF method. A local electrostatic potential formed by the  $1s$  and  $2s$  spectator orbitals,  $2v_0(1s,r) + v_0(2s,r)$  [49], is considered in all active orbitals, where  $v_0(v,r)$  is given by

$$v_0(v,r) = \int [P_v(r')^2 + Q_v(r')^2] \frac{1}{r_{>}} dr'. \quad (4)$$

Here  $P_v$  and  $Q_v$  are the large and small components of the radial wave functions of a spectator orbital  $v$  and  $r_{>} = \max(r,r')$ . A comparison with the spectator orbitals of all states obtained with the MCDF code shows differences of the order of 5%, which can be neglected for the evaluation of the electrostatic potential. The spectator orbitals of the  $2s2p^3 P_0$  state are chosen for  $v_0(1s,r)$  and  $v_0(2s,r)$ . A local statistical-exchange potential is also included in order to approximate the nonlocal part of the Dirac-Fock equation. We follow the original procedure of Cowan [50] that defines this local potential for an orbital  $v$  as

$$v_{\text{exc}}(v,r) = -k_1 \phi(r) \left[ \frac{\rho'(r)}{\rho'(r) + 0.5/(n_\nu - l_\nu)} \right] \times \left( \frac{\rho'(r)}{\rho(r)} \right) \left( \frac{24\rho(r)}{\pi} \right)^{1/3}, \quad (5)$$

where  $\rho$  is the many-electron total electron density and  $\rho'(r)$  is the modified total density without the contribution of the  $v$  orbital, i.e.,  $\rho'(r) = \rho(r) - \min(2, e_\nu) \rho_\nu(r)$ , with  $\rho_\nu(r)$  being the electron density of the orbital  $v$ . The quantity  $e_\nu$  is the number of equivalent electrons at the orbital  $v$  with principal quantum number and orbital angular momentum  $n_\nu$  and  $l_\nu$ ,

TABLE I. Optimal values of  $k_1$  and energy differences (eV). The energy of the initial state  $2s2p^3 P_0$  is relative to the final state  $2s^2 1S_0$  ( $\omega_t$ ), while the rest are relative to the initial state  $E_n - E_{2s2p^3 P_0}$ . We list the energy differences obtained by the FBS method without  $k_1$  optimization ( $E_{\text{FBS}}^*$ ) and with  $k_1$  optimization, which are equal (in the quoted precision) to the ones obtained by the MCDF method ( $E_{\text{MCDF}}$ ). Values provided by Ref. [51] are also listed.

State	$k_1$	$E_{\text{FBS}}^*$	$E_{\text{MCDF}}$	Ref. [51]
Xe <sup>50+</sup>				
$3P_0 - 1S_0$	0.79	118.5	104.1	104.5
$3P_1 - 3P_0$	0.64	0.0	23.9	22.8
$1P_1 - 3P_0$	0.62	400.8	430.1	428.3
U <sup>88+</sup>				
$3P_0 - 1S_0$	0.69	252.7	258.1	258.3
$3P_1 - 3P_0$	0.58	0.0	41.6	39.9
$1P_1 - 3P_0$	0.72	4259.3	4245.3	4243.3

respectively. The function  $\phi(r)$  takes into account the different influence of the centrifugal potential to the various orbitals as described in Ref. [50]. All the present wave functions and densities necessary for calculating Eqs. (4) and (5) were obtained by the MCDF method.

Next we identify the intermediate states with the most relevant weight to the summations and calculate their most accurate MCDF energies  $E_n$ . These intermediate states are depicted in Fig. 1. While the parameter  $k_1$  is set to 0.7 in Ref. [50] as the best empirical guess for the exchange potential, we here consider it as a free parameter. Optimal values of this parameter are obtained by comparing the values of the transition energy  $\omega_t$  and the energy differences  $E_n - E_{2s2p^3 P_0}$  [denominators of Eq. (3)], obtained by the FBS method and with the respective ones of the MCDF method. Table I lists the optimal values of  $k_1$  that minimizes the differences between the FBS and MCDF of the mentioned energy differences.

The MCDF calculations were performed using the general relativistic MCDF code (MDFGME) [52].

Calculations of the decay rate were performed in both length and velocity gauges. The quality of the evaluation of the two-photon amplitudes is directly connected to the gauge invariance, under the premise that the potential remains local in all states [11,48]. Although we introduced different local-exchange potentials in the states and MCDF energies, we notice that the gauge invariance is still at a level of few percent.

With the application of the present formalism to the decay of  $1s2p^3 P_0$  to  $1s^2 1S_0$  in heliumlike ions, and with an effective potential of  $v_0(1s,r)$ , we reproduce the results of Ref. [45] within the respective accuracy.

## III. RESULTS AND DISCUSSION

The results of our calculations for the  $2s2p^3 P_0 \rightarrow 2s^2 1S_0$   $E1M1$  decay rate  $W$  are presented in Table II. The lifetimes that we obtained, correspond to  $\sim 3$  min and 12 s for Xe<sup>50+</sup> and U<sup>88+</sup> ions, respectively. Other allowed higher-order multipole contributions to this transition, like the  $E2M2$  or  $E3M3$ , are severely reduced. The value obtained for the  $E2M2$

TABLE II. Decay rate ( $s^{-1}$ ) for the  $2s2p\ ^3P_0 \rightarrow 2s^2\ ^1S_0\ E1M1$  transition in xenon and uranium. Relativistic calculations have been performed in velocity  $V$  and length  $L$  gauges for several cases: with ( $W^{\text{opt}}$ ) and without ( $W^{\text{nonopt}}$ )  $k_1$  optimization, with the summation carried without negative energies ( $W^+$ ), having the energies provided by Ref. [51] ( $W^*$ ), and without the effective exchange potential ( $W^{\text{noexc}}$ ).

Ion	$W_V^{\text{opt}}$	$W_L^{\text{opt}}$	$W_V^{\text{nonopt}}$	$W_L^{\text{nonopt}}$	$W_V^+$	$W_L^+$	$W_V^*$	$W_L^*$	$W^{\text{noexc}}$
Xe <sup>50+</sup>	$4.78 \times 10^{-3}$	$4.97 \times 10^{-3}$	$4.05 \times 10^{-3}$	$4.05 \times 10^{-3}$	$4.78 \times 10^{-3}$	$4.98 \times 10^{-3}$	$5.20 \times 10^{-3}$	$5.40 \times 10^{-3}$	$5.30 \times 10^{-3}$
U <sup>88+</sup>	$8.04 \times 10^{-2}$	$8.06 \times 10^{-2}$	$9.35 \times 10^{-2}$	$9.35 \times 10^{-2}$	$8.08 \times 10^{-2}$	$8.11 \times 10^{-2}$	$8.18 \times 10^{-2}$	$8.20 \times 10^{-2}$	$8.31 \times 10^{-2}$

decay rate in berylliumlike uranium,  $8.2 \times 10^{-18}\ s^{-1}$  shows its negligible impact on the total decay rate.

Calculations were performed in both velocity and length gauges, showing differences of up to 4% due to the different local-exchange potentials in the states. A calculation without these effective exchange potentials ( $W^{\text{no-exc}}$ ) results in a gauge invariance of  $10^{-10}\%$ .

Differences between the values of the decay rate with ( $W^{\text{opt}}$ ) and without  $k_1$ -optimization ( $W^{\text{non-opt}}$ ) in Table III are mostly due to the respective transition energies, on which the decay rate depends quadratically, as well on the different between  $^3P_1$  and  $^1P_1$  energies. These values can also be compared with the case of not considering the effective exchange potential of Eq. (5). Differences of up to 20% and 16% in xenon and uranium, respectively, shows how sensitive the decay of this transition is to the electronic correlation, in particular to the non-local part of the electron-electron interaction.

Residual differences of 0.5–2 eV between MCDHF energy values and those of Ref. [51] results in relative differences of 8% in the decay rate ( $W^*$ ). Most of the experimental observations [27,53,54] and theoretical calculations [51,55–58] of these energies are included in a energy range of 2 eV, resulting in differences up to 10%.

In contrast to previous studies of the negative continuum, where it was shown that its contribution has to be included in relativistic calculations of two-photon decay rates [35,36] and one-photon decay rates [37,38], they contribute by only a few percent to the present case, even for berylliumlike uranium ions. Following the semirelativistic approach of Ref. [45], the estimation of the negative-continuum contribution to the decay of  $p \rightarrow s\ E1M1$  transitions is proportional to  $\omega_i^5/Z^2$ . Previous studies deal with transitions between principal quantum numbers (e.g. [36]), for which the transitions energies scale as  $Z^4$ . In the present case, the transition addresses the same quantum number and scales roughly as  $Z$  for berylliumlike uranium. This explain the observed smaller contribution of the negative energy continuum on the total decay rate.

To be conservative, we consider the uncertainty in the decay rate as the combined uncertainty of the previous effects and the final result having the  $k_1$  optimization. The final decay of

TABLE III. Comparison between our final value of the decay rate  $W$  ( $s^{-1}$ ) and values provided by Refs. [26,43]. Reference [26] is an extension of Ref. [43] by taking the energy splitting  $^3P_0 - ^3P_1$  into account.

Ion	$W$	Ref. [43]	Ref. [26]
Xe <sup>50+</sup>	$(5 \pm 1) \times 10^{-3}$	$3.4 \times 10^{-2}$	$5.2 \times 10^{-2}$
U <sup>88+</sup>	$(8 \pm 1) \times 10^{-2}$	$2.6 \times 10^1$	$4.9 \times 10^1$

the  $E1M1$  decay rate is thus equal to  $(5 \pm 1) \times 10^{-3}\ s^{-1}$  and  $(8 \pm 1) \times 10^{-2}\ s^{-1}$  for xenon and uranium, respectively.

We notice evident differences relative to previous calculations listed in Table III by factors from 10 to 300. The differences can be attributed to our fully relativistic approach in a  $jj$ -coupling scheme. The values of Refs. [42,43] were obtained by considering only the  $2s2p\ ^3P_1$  and  $2s2p\ ^1P_1$  states in the intermediate-state summation and were calculated in a non-relativistic  $LS$ -coupling framework. Moreover, the non-relativistic form of the electric and magnetic dipole operators was also employed in Refs. [42,43], which forbids intercombination transitions with a spin-flip of the total spin in a  $LS$ -coupling. Therefore, spin-orbit and spin-spin interactions were included in first approximation in order to mix the  $^3P_1$  and  $^1P_1$  terms. For highly charged ions, intercombination transitions are allowed in a  $jj$ -coupling scheme with relativistic wavefunctions, as the spin-orbit interaction is already included nonperturbatively. Other investigations of the  $E1E1$  have shown that relativistic effects increase the decay rate by 30% [12,59] in heliumlike Xe. In the present case, the  $M1$  mode is even more sensitive to the  $LS$ -coupling scheme that is not appropriate for highly charged ions, where the strong spin-orbit interaction is included perturbatively. A similar factor of 300 was already obtained in a relativistic calculation [60].

#### IV. CONCLUSION

We have presented the results of the two-photon forbidden  $E1M1$  decay rate for two selected heavy elements obtained with an effective potential. The limitations of the single configuration model for this particular decay are investigated and found that while this approach cannot be applied to low- and middle- $Z$  ions, for berylliumlike Xe and heavier elements, each state is well described by a single CSF with orthogonal orbitals. Therefore, excitations of the spectator electron that forbid the use of this model can be neglected. We have found a negligible contribution of negative-energy states to this decay rate, which is in agreement with semirelativistic estimations. Not unexpectedly, we observe significant relativistic effects relative to previous non-relativistic calculations performed for these transitions. These transitions in middle  $Z$  ions may have been observed and their rates might be experimentally measurable, or at least estimated approximately, in the near future.

#### ACKNOWLEDGMENTS

This research was supported in part by Fundação para a Ciência e a Tecnologia (FCT), Portugal, through Project No. PTDC/FIS/117606/2010, financed by the European Community Fund FEDER through the COMPETE. P.A., J.M., and M.G. acknowledge support from FCT, under Contracts No. SFRH/BPD/92329/2013, No. SFRH/BD/52332/2013, and No.

SFRH/BPD/92455/2013. F.F. acknowledges support from the Austrian Science Fund through START Grant No. Y 591-N16. L.S. acknowledges financial support from the People Programme (Marie Curie Actions) of the European Union's Seventh Framework Programme (Program No. FP7/2007-2013) under REA Grant Agreement No. 291734. P.I. acknowledges the support as a Helmholtz Alliance HA216/EMMI member. Laboratoire Kastler Brossel is "UMR n° 8552" of the École Normale Supérieure, CNRS, Collège de France and Sorbonne University - Universiy Pierre and Marie Curie-Paris 06.

**APPENDIX : REDUCED MATRIX ELEMENTS**

Within the AEM, both initial, intermediate and final states are described by a single CSF. With this assumption, and following the treatment given in [11,14], we arrive at Eqs. (2) and (3), with the reduced matrix elements between two orbitals  $\alpha$  and  $\beta$  being given by

$$\langle \alpha || R || \beta \rangle = \sqrt{\frac{4\pi [j_\alpha, j_\beta]}{\sqrt{3}}} \begin{pmatrix} j_\alpha & 1 & j_\beta \\ 1/2 & 0 & -1/2 \end{pmatrix} \times \begin{Bmatrix} J_\alpha & 1 & J_\beta \\ j_\beta & 1/2 & j_\alpha \end{Bmatrix} \overline{M}^R(\omega). \quad (A1)$$

For the relativistic dipole magnetic multipole [ $R \equiv M_1(\omega)$ ], the radial part  $\overline{M}$  is written as

$$\overline{M}^{M_1}(\omega) = \frac{3}{\sqrt{2}}(\kappa_\alpha + \kappa_\beta)I_1^+, \quad (A2)$$

whereas for the relativistic electric dipole multipole, the two radial part components [ $R \equiv E_1^{\lambda=-1,1}(\omega)$ ] are given by

$$\overline{M}^{E_1^{-1}}(\omega) = G[3J^{(1)} + (\kappa_f - \kappa_i)(I_2^+ + I_0^+) - I_0^- + 2I_2^-], \quad (A3)$$

and

$$\overline{M}^{E_1^1}(\omega) = \frac{1}{\sqrt{2}}[(\kappa_f - \kappa_i)I_2^+ + 2I_2^-] - \sqrt{2}[(\kappa_f - \kappa_i)I_0^+ - I_0^-]. \quad (A4)$$

The quantum numbers  $j$ ,  $J$  and  $\kappa$  refers to the electron total angular momentum, state total angular momentum and relativistic number.  $G$  is a gauge parameter that in velocity and length gauges is equal to 0 and  $\sqrt{2}$ , respectively. The radial integrals  $J^{(1)}$  and  $I_L^\pm$  are given as in Refs. [11,44].

---

[1] M. Göppert-Mayer, Über elementarakte mit zwei quantensprüngen, *Ann. Phys. (Leipzig)* **401**, 273 (1931).

[2] J. Shapiro and G. Breit, Metastability of  $2s$  states of hydrogenic atoms, *Phys. Rev.* **113**, 179 (1959).

[3] R. Marrus and R. W. Schmieder, Forbidden decays of hydrogenlike and heliumlike argon, *Phys. Rev. A* **5**, 1160 (1972).

[4] V. Florescu, Two-photon emission in the  $3s \rightarrow 1s$  and  $3d \rightarrow 1s$  transitions of hydrogenlike atoms, *Phys. Rev. A* **30**, 2441 (1984).

[5] C. K. Au, Effect of higher multipole transitions in the two-photon decay spectrum of metastable hydrogen, *Phys. Rev. A* **14**, 531 (1976).

[6] A. Aspect, J. Dalibard, and G. Roger, Experimental Test of Bell's Inequalities Using Time-Varying Analyzers, *Phys. Rev. Lett.* **49**, 1804 (1982).

[7] H. Kleinpoppen, A. J. Duncan, H. J. Beyer, and Z. A. Sheikh, Coherence and polarization analysis of the two-photon radiation of metastable atomic hydrogen, *Phys. Scr.* **72**, 7 (1997).

[8] F. Fratini, M. C. Tichy, T. Jahrsetz, A. Buchleitner, S. Fritzsche, and A. Surzhykov, Quantum correlations in the two-photon decay of few-electron ions, *Phys. Rev. A* **83**, 032506 (2011).

[9] L. Safari, P. Amaro, J. P. Santos, and F. Fratini, Angular and polarization analysis for two-photon decay of  $2s$  hyperfine states of hydrogenlike uranium, *Phys. Rev. A* **90**, 014502 (2014).

[10] C. Schwob, L. Jozefowski, B. de Beauvoir, L. Hilico, F. Nez, L. Julien, F. Biraben, O. Acef, J. J. Zondy, and A. Clairon, Optical Frequency Measurement of the  $2s$ - $12d$  Transitions in Hydrogen and Deuterium: Rydberg Constant and Lamb Shift Determinations, *Phys. Rev. Lett.* **82**, 4960 (1999).

[11] S. P. Goldman and G. W. F. Drake, Relativistic two-photon decay rates of  $2s_{1/2}$  hydrogenic ions, *Phys. Rev. A* **24**, 183 (1981).

[12] A. Derevianko and W. R. Johnson, Two-photon decay of  $2^1S_0$  and  $2^3S_1$  states of heliumlike ions, *Phys. Rev. A* **56**, 1288 (1997).

[13] S. Trotsenko *et al.*, Spectral shape of the Two-Photon Decay of the  $2^1S_0$  State in He-like Tin, *Phys. Rev. Lett.* **104**, 033001 (2010).

[14] R. W. Dunford, M. Hass, E. Bakke, H. G. Berry, C. J. Liu, M. L. A. Raphaelian, and L. J. Curtis, Lifetime of Two-Photon Emitting States in Heliumlike and Hydrogenlike Nickel, *Phys. Rev. Lett.* **62**, 2809 (1989).

[15] E. Träbert, E1-forbidden transition rates in ions of astrophysical interest, *Phys. Scr.* **89**, 114003 (2014).

[16] E. Träbert and G. Gwinner, ( $M1 + E2$ ) decay rate in  $\text{Ar}^{2+}$  ions measured at a heavy-ion storage ring, *Phys. Rev. A* **65**, 014501 (2001).

[17] E. Träbert, P. Beiersdorfer, G. Gwinner, E. H. Pinnington, and A. Wolf,  $M1$  transition rate in  $\text{Cl}^{12+}$  from an electron-beam ion trap and heavy-ion storage ring, *Phys. Rev. A* **66**, 052507 (2002).

[18] T. Brage, P. G. Judge, A. Aboussaïd, M. R. Godefroid, P. Jönsson, A. Ynnerman, C. F. Fischer, and D. S. Leckrone, Hyperfine induced transitions as diagnostics of isotopic composition and densities of low-density plasmas, *Astrophys. J.* **500**, 507 (1998).

[19] T. Brage, P. G. Judge, and C. R. Proffitt, Determination of Hyperfine-Induced Transition Rates from Observations of a Planetary Nebula, *Phys. Rev. Lett.* **89**, 281101 (2002).

[20] C. W. Allen, *Astrophysical Quantities* (Athlone, London, 1973).

[21] K. J. H. Phillips, J. Sylwester, B. Sylwester, and E. Landi, Solar flare abundances of potassium, argon, and sulphur, *Astrophys. J.* **589**, L113 (2003).

- [22] M. Maul, A. Schäfer, W. Greiner, and P. Indelicato, Prospects for parity-nonconservation experiments with highly charged heavy ions, *Phys. Rev. A* **53**, 3915 (1996).
- [23] M. Maul, A. Schäfer, and P. Indelicato, Stark quenching for the  $1s^2 2s 2p^3 P_0$  level in beryllium-like ions and parity-violating effects, *J. Phys. B* **31**, 2725 (1998).
- [24] M. Guerra, P. Amaro, C. I. Szabo, A. Gumberidze, P. Indelicato, and J. P. Santos, Analysis of the charge state distribution in an ECRIS Ar plasma using high-resolution x-ray spectra, *J. Phys. B* **46**, 065701 (2013).
- [25] E. A. Alden, K. R. Moore, and A. E. Leanhardt, Two-photon  $E1$ - $M1$  optical clock, *Phys. Rev. A* **90**, 012523 (2014).
- [26] D. Bernhardt, C. Brandau, C. Kozhuharov, A. Müller, S. Schippers, S. Böhm, F. Bosch, J. Jacobi, S. Kieslich, H. Knopp, P. H. Mokler, F. Nolden, W. Shi, Z. Stachura, M. Steck, and T. Stöhlker, Towards a measurement of the  $2s 2p^3 P_0 \rightarrow 2s^2 ^1S_0$   $E1M1$  two photon transition rate in Be-like xenon ions, *J. Phys.: Conf. Ser.* **388**, 012007 (2012).
- [27] D. Bernhardt, C. Brandau, Z. Harman, C. Kozhuharov, S. Böhm, F. Bosch, S. Fritzsche, J. Jacobi, S. Kieslich, H. Knopp, F. Nolden, W. Shi, Z. Stachura, M. Steck, T. Stöhlker, S. Schippers, and A. Müller, Spectroscopy of berylliumlike xenon ions using dielectronic recombination, *J. Phys. B* **48**, 144008 (2015).
- [28] J. P. Marques, F. Parente, and P. Indelicato, Hyperfine quenching of the  $1s^2 2s 2p^3 P_0$  level in berylliumlike ions, *Phys. Rev. A* **47**, 929 (1993).
- [29] K. T. Cheng, M. H. Chen, and W. R. Johnson, Hyperfine quenching of the  $2s 2p^3 P_0$  state of berylliumlike ions, *Phys. Rev. A* **77**, 052504 (2008).
- [30] M. Andersson, Y. Zou, R. Hutton, and T. Brage, Hyperfine-dependent lifetimes in Be-like ions, *Phys. Rev. A* **79**, 032501 (2009).
- [31] S. Schippers, E. W. Schmidt, D. Bernhardt, D. Yu, A. Müller, M. Lestinsky, D. A. Orlov, M. Grieser, R. Repnow, and A. Wolf, Storage-Ring Measurement of the Hyperfine Induced  $^{47}\text{Ti}^{18+}(2s 2p^3 P_0 \rightarrow 2s^2 ^1S_0)$  Transition Rate, *Phys. Rev. Lett.* **98**, 033001 (2007).
- [32] S. Schippers, D. Bernhardt, A. Müller, M. Lestinsky, M. Hahn, O. Novotný, D. W. Savin, M. Grieser, C. Krantz, R. Repnow, and A. Wolf, Storage-ring measurement of the hyperfine-induced  $2s 2p^3 P_0 \rightarrow 2s^2 ^1S_0$  transition rate in berylliumlike sulfur, *Phys. Rev. A* **85**, 012513 (2012).
- [33] W. R. Johnson, Hyperfine quenching: review of experiment and theory, *Can. J. Phys.* **89**, 429 (2011).
- [34] J. Grumer, W. Li, D. Bernhardt, J. Li, S. Schippers, T. Brage, P. Jönsson, R. Hutton, and Y. Zou, Effect of an external magnetic field on the determination of  $E1M1$  two-photon decay rates in Be-like ions, *Phys. Rev. A* **88**, 022513 (2013).
- [35] L. N. Labzowsky, A. V. Shonin, and D. A. Solov'yev, QED calculation of  $E1M1$  and  $E1E2$  transition probabilities in one-electron ions with arbitrary nuclear charge, *J. Phys. B* **38**, 265 (2005).
- [36] A. Surzhykov, J. P. Santos, P. Amaro, and P. Indelicato, Negative-continuum effects on the two-photon decay rates of hydrogenlike ions, *Phys. Rev. A* **80**, 052511 (2009).
- [37] A. Derevianko, I. M. Savukov, W. R. Johnson, and D. R. Plante, Negative-energy contributions to transition amplitudes in heliumlike ions, *Phys. Rev. A* **58**, 4453 (1998).
- [38] P. Indelicato, Correlation and Negative Continuum Effects for the Relativistic  $M1$  Transition in Two-Electron Ions Using the Multiconfiguration Dirac-Fock Method, *Phys. Rev. Lett.* **77**, 3323 (1996).
- [39] U. I. Safronova, W. R. Johnson, M. S. Safronova, and A. Derevianko, Relativistic many-body calculations of transition probabilities for the  $2l_1 2l_2 [LSJ] - 2l_3 2l_4 [L'S'J']$  lines in Be-like ions, *Phys. Scr.* **59**, 286 (1999).
- [40] M. H. Chen, K. T. Cheng, and W. R. Johnson, Large-scale relativistic configuration-interaction calculation of the  $2s^2 ^1S_0 - 2s 2p^3 P_1$  intercombination transition in C III, *Phys. Rev. A* **64**, 042507 (2001).
- [41] P. Indelicato, V. M. Shabaev, and A. V. Volotka, Interelectronic-interaction effect on the transition probability in high- $Z$  He-like ions, *Phys. Rev. A* **69**, 062506 (2004).
- [42] R. W. Schmieder, Double- and triple-photon decay of metastable  $^3P_0$  atomic states, *Phys. Rev. A* **7**, 1458 (1973).
- [43] C. Laughlin, Radiative decay of the  $2^3P_0^o$  level of beryllium-like ions, *Phys. Lett.* **75A**, 199 (1980).
- [44] J. P. Santos, P. Patte, F. Parente, and P. Indelicato, Spontaneous relativistic two-photon decay rate mathematical expression in heliumlike systems, *Eur. Phys. J. D* **13**, 27 (2001).
- [45] I. M. Savukov and W. R. Johnson, Two-photon  $E1M1$  decay of  $2^3P_0$  states in heavy heliumlike ions, *Phys. Rev. A* **66**, 062507 (2002).
- [46] A. I. Akhiezer and V. B. Berestetskii, *Quantum Electrodynamics* (Interscience, New York, 1965).
- [47] J. P. Santos, F. Parente, and P. Indelicato, Application of B-splines finite basis sets to relativistic two-photon decay rates of  $2s$  level in hydrogenic ions, *Eur. Phys. J. D* **3**, 43 (1998).
- [48] P. Amaro, J. P. Santos, F. Parente, A. Surzhykov, and P. Indelicato, Resonance effects on the two-photon emission from hydrogenic ions, *Phys. Rev. A* **79**, 062504 (2009).
- [49] W. Johnson, *Atomic Structure Theory: Lectures on Atomic Physics* (Springer, New York, 2007).
- [50] R. D. Cowan, Atomic self-consistent-field calculations using statistical approximations for exchange and correlation, *Phys. Rev.* **163**, 54 (1967).
- [51] M. S. Safronova, W. R. Johnson, and U. I. Safronova, Relativistic many-body calculations of the energies of the  $n = 2$  states for the berylliumlike isoelectronic sequence, *Phys. Rev. A* **53**, 4036 (1996).
- [52] P. Indelicato and J. P. Desclaux, Multiconfiguration Dirac-Fock calculations of transition energies with QED corrections in three-electron ions, *Phys. Rev. A* **42**, 5139 (1990).
- [53] D. Feili, B. Zimmermann, C. Neacsu, P. Bosselmann, K. H. Schartner, F. Folkmann, A. E. Livingston, E. Träbert, and P. H. Mokler,  $2s^2 ^1S_0 - 2s 2p^3 P_1$  intercombination transition wavelengths in Be-like  $\text{Ag}^{43+}$ ,  $\text{Sn}^{46+}$ , and  $\text{Xe}^{50+}$  ions, *Phys. Scr.* **71**, 48 (2005).
- [54] P. Beiersdorfer, D. Knapp, R. E. Marrs, S. R. Elliott, and M. H. Chen, Structure and Lamb-Shift of  $2s_{1/2} - 2p_{3/2}$  Levels in Lithiumlike  $\text{U}^{89+}$  Through Neonlike  $\text{U}^{82+}$ , *Phys. Rev. Lett.* **71**, 3939 (1993).
- [55] M. H. Chen and K. T. Cheng, Energy levels of the ground state and the  $2s 2pn$  ( $j = 1$ ) excited states of berylliumlike ions: A large-scale, relativistic configuration-interaction calculation, *Phys. Rev. A* **55**, 166 (1997).

- [56] J. P. Santos, J. P. Marques, F. Parente, E. Lindroth, S. Boucard, and P. Indelicato, Multiconfiguration Dirac-Fock calculation of  $2s_{1/2}$ - $2p_{3/2}$  transition energies in highly ionized bismuth, thorium, and uranium, *Eur. Phys. J. D* **1**, 149 (1998).
- [57] U. I. Safronova, Excitation energies and transition rates in Be-, Mg-, and Zn-like ions, *Mol. Phys.* **98**, 1213 (2000).
- [58] K. T. Cheng, M. H. Chen, and J. Sapirstein, Quantum electrodynamic corrections in high- $Z$  Li-like and Be-like ions, *Phys. Rev. A* **62**, 054501 (2000).
- [59] G. W. F. Drake, Spontaneous two-photon decay rates in hydrogenlike and heliumlike ions, *Phys. Rev. A* **34**, 2871 (1986).
- [60] F. Fratini (private communication).